

A Momentum Exchange Flexible Debris-Sweeper System: An Ambitious Proposal to Mitigate the Global Space Debris Problem

Mahan Behroo¹, Assadian N.² and Last Author³

1. Department of aerospace engineering, Sharif University of Technology, Tehran, Iran
2. Department of aerospace engineering, Sharif University of Technology, Tehran, Iran
3. E-mail any correspondence to: myname@domain.com

Abstract

This study aims to propose a method of utilizing an orbital device based on contact momentum exchange, to divert the trajectories of several debris objects in succession. This Spacecraft consists of four thruster modules, all connected through a square rigid frame enclosing a flexible membrane. By coordinating the thrust on the modules, the central portion of membrane can be used as a momentum exchange contact medium. This way the delta-v required to de-orbit the debris object can be delivered and the perigee can be lowered to the point that the earth atmospheric decay takes over. Dynamics of such flexible multi-body system is studied by utilizing a lumped-mass parameter model in order to investigate the feasibility of the proposed method and considering the implications regarding its design...

Keywords: Active Debris Removal, Momentum Exchange, Flexible

Introduction

The issue of congested orbital area due to the existence of space debris is well established among the space research community. since 2003, as a result of purposeful explosion of a Chinese satellite and later in 2009, in the aftermath of the Cosmos-Iridium collision, great threat of the cascading effect has become increasingly clear [1]. Such fragmentation introduces the probability of huge future costs associated with shrapnel impact with functional objects in orbit. Based on information available from those events, the so called "hidden" loss happens when a shard impacts with a satellite a decade after the original incident [2]. As of 2009, European Space Agency led the efforts to identify and catalogue debris

objects in orbit. This program is being carried out as part of the space situational awareness program (SSA). Currently, IADS (Inter-Agency Space Debris Coordination committee) requires all new missions meant for operation in LEO to incorporate an end of life termination scheme, to de-orbit the satellite in a 25 years period [3]. Moreover, Geostationary satellites are required by ITU (International Telecommunication Union) to move to a graveyard orbit at the end of their mission [4].

Based on projections made by computer models, it has been concluded that the implementation of the "25-year rule" could in fact be conducive to preventing long term growth of LEO space debris population. Regardless of these mitigation agenda, a great majority of in-orbit satellites are decommissioned and experiencing the end of mission phase, with no means of leaving the earth orbit in a foreseeable future. That is why, there is a dire need for implementing debris removal methods as soon as possible, otherwise the problem could prove to be insurmountable. A wide range of methods have been proposed to deal with the problem. The principle is to somehow dissipate the object's orbital energy. Many of the proposed methods are actually based on the momentum exchange principle. Apart from non-contact diversion methods, such as the ion-beam [5], laser impulse bombardment [6], or Geo-magnetic approach [7], other momentum exchange methods rely on utilizing nets [8, 9, 10], harpoons or robotic arms [11] to initiate physical contact and capture the debris object. Another suggested approach is to enhance the drag imposed on the debris by using expanding foam to increase the cross section [12]. While non-contact methods prove to be more effective for small sized objects, it is impractical to use them for larger

objects like defunct satellites.

Comprehensive studies regarding the various removal methods and means to compare and cross analysis of them are carried out in [14, 15, 16, 13, 17].

A widely accepted notion of the catalogued debris objects, classifies them into three groups. These groups entail the small objects ($< 1\text{cm}$), medium objects (1 to 10cm) and large objects ($> 10\text{cm}$). The population of these objects increase as they become smaller in size. despite the smaller number of heavy debris objects, the priority is to remove them first, as each of them could spark another catastrophic fragmentation event. The urgency of removing smaller objects diminishes as the object mass becomes smaller. Moreover, shielding can be applied to reduce the vulnerability of satellites and space stations against smaller fragments. By definition, all active debris removal methods are limited in terms of diversity of the objects they intend to remove. Physical contact removal methods are mainly focused on large to medium objects. The spacecraft in this study is also meant for targeting large objects. The proposed system aims at de-orbiting multiple objects in a successive manner. Once the device gets to orbit, it can go from one debris object to another, sweeping each object by changing its transnational momentum in a favoured manner. Normally, for removal of medium to large objects, the remover spacecraft is required to engage in a proximity maneuvering scenario. Such proximity maneuvers may entail various phases such as attitude synchronization, capture, de-tumbling and at last deploying the removal agent itself. The removal agent could be a net, thruster or any other proposed device. The aforementioned sequence of maneuvers are costly in terms of technology complexity and fuel efficiency associated with the removal method.

Mission and Methods Description

The most prominent implication of all physical contact removal methods is that in terms of reducing the future costs and risks of the debris congested area, such missions seem to be effective only to a small degree.

Some authors proposed the possibility of consecutive removal agenda, where a spacecraft or a fleet, moves through orbits to rendezvous with multiple debris objects. It is indeed intuitive to assume that a characteristic for a successful removal method is the ability of the sweeper spacecraft to move through pre-calculated optimized path in order to remove more than one object from orbit. Levin proposed such mission as a "wholesale" removal method, in which a fleet of electrodynamics tether devices wander in earth orbit to remove multiple targets [18]. Many works suggest a single spacecraft to carry out the mission and propose specific strategies to accomplish the momentum exchange. Missel and Mortari explored the possibility of utilizing the momentum exchange phenomena to reduce

the fuel requirements of the proposed mission [19]. Such an approach consists of a mission profile in which a single sweeper device moves from one debris object to another, using the change in momentum to reach the next target. This assumption generally leads to designs incorporating a tether based capture [20], since such momentum harnessing requires a long arm or a tether [22, 27, 23, 26, 24, 25, 21]. It is worth noting that the effectiveness and feasibility of such proposals are yet to be confirmed and the concept itself requires further research. However, the necessity of such consecutive mission agenda is beyond any reasonable doubt. One important issue to address is that previous designs tend to either underestimate or oversimplify the overall complexity of the consecutive captures and ejections. In reality, the process of capture requires some sort of stabilizing strategy in order to secure the object. This can be achieved by utilizing nets or arms, however, it is extremely hard to get a grip of a non-cooperative object in space, in such fashion that it can also be easily ejected out. Moreover, every net introduces the possibility of multiple areas of entanglement with the object. Robotic arms and grippers also have tough time securing the objects with different shapes. It can be argued that the capture net can be ejected with the object, however, this dictates the need for spare net and capture equipment for every single object, which doesn't seem to be feasible. In addition, utilizing long tethers to harness the momentum differential, becomes more economically efficient the longer the tether is. It is evident that longer tethers are harder to deploy and control, and in case of failures, a long tether can be more dangerous than the debris it was supposed to remove.

Such issues are not discussed in previously mentioned works and assumptions are made to allow solutions for multiple removal missions. Apart from these issues, the most important factor in planning such missions is the fuel consumption of the whole scheme. There is a great cost associated with the orbital maneuvers conducive to the rendezvous process. Moreover, the de-orbit burn, if exists, also consumes considerable amount of fuel. In considering the problem of space debris removal, it would not be far fetched to plan for orbital refuelling. In general, future space endeavors will use parking orbits more extensively and planning moon and mars colonization schemes, certainly merits the existence of such refuelling modules in future. On-orbit servicing is a technology already in use [28], and regarded as a necessity [29]. The possibility of such depot-based space transportation system has already been discussed and studied [30]. As a result, at least in theory, it can be assumed that the sweeper spacecraft could potentially refuel in orbit to continue its mission beyond the limits dictated by its embedded capabilities at launch.

Proposed Design and Diversion Method

Based on previously mentioned remarks, this section presents elements of a novel debris removal system. The design is meant to be effective in terms of delta-v delivery capacity and also to address the complexities associated with consecutive removals. Contrary to previously mentioned methods, here, the desired momentum exchange is delivered through contact force. As a result, there is no need for a net, gripper or towing and the spacecraft simply pushes the object during thrust deployment. This way, adhesion vulnerabilities are remediated and the spacecraft can potentially carry out a consecutive removal mission in a reliable manner. The sweeper spacecraft depicted in Figure 1 consists of four thruster modules, connected together through a rigid frame. The flexible membrane at the center acts as the contact medium with the debris object.

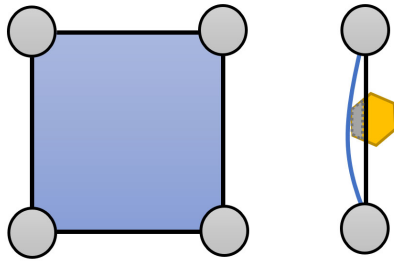


Figure 1: Left: Sweeper spacecraft in original configuration, Right: Sweeper spacecraft moving along with the debris object.

At the start of the mission, the sweeper spacecraft (ssc) is stationed in its parking orbit waiting to receive confirmation of a designated target debris. Upon receiving a valid target, the spacecraft starts performing a plane change maneuver to enter the orbital plane of the designated debris object (ddo). Then, the ssc starts performing a hohman transfer using two consecutive burns, aligning its orbit with that of the ddo. This hohman transfer effectively acts as a rendezvous transfer and sets up the ssc for removal of the ddo at the ddo's perigee. This rendezvous maneuver is carried out in a way to ensure that ssc arrives at destination ahead of the ddo and not trailing it. This way, after the second hohman burn, the ssc can be tuned to exist in a frame, being approached by the ddo with small relative velocity, while maintaining fuel efficiency. The process of removal starts where the ddo is approaching to touch the center of the flexible membrane.

Upon surface contact, the membrane experiences local deformations due to the presence of contact force. Here, the modules produce desirable thrust in order to keep the ddo at the center of the membrane and at the same time limiting the maximum allowable deformation. Granted that the membrane has proper damping attribute, it is possible to reach an state of equilibrium in which the ssc and the ddo move together, and the membrane is slightly

deformed. This state requires a finite amount of thrust that should be applied at the modules.

At this stage, the main segment of the mission starts. While the membrane is in contact with the object, the modules activate the most important burn of the mission, namely, the de-orbit burn. The de-orbit burn starts to counter the orbital velocity of the companions and given enough thrust force through contact time, the ddo's orbital velocity starts to decrease. As soon as the de-orbit criteria for the ddo is met, the ssc starts performing departure. In this segment, modules simply cancel the thrust. By that virtue, the energy imposed by the contact force during these last seconds will shoot the ddo away from the ssc, due to the potential energy stored in the membrane. Now, the de-orbit process is accomplished and the ddo ends up in a new orbit with significantly lower perigee, dictating its de-orbit into the desired time frame. Now, the ssc is occupying almost the same orbit (apart from the obvious last kick that separated the agents), so it will have to move to another orbit to rendezvous with the next ddo, or at least keep itself away from that low perigee orbit. In any case, the ssc waits for another confirmed ddo and continues to clean LEO until it runs out of fuel or hypothetically rendezvous with a space tanker.

Physics

The proposed design incorporates complex physical phenomena such as orbital synchronization maneuvers and multiple instances of contact between rigid and flexible objects. The objects experience impact with small relative velocity so proper control logic must be utilized to smoothly exchange momentum while keeping the contact. In this section, a breakdown of such phenomena are presented and equations of motion for the multi-body system are derived with the goal of paving the way for producing a computer simulation and understanding the dynamics of the system.

Momentum Exchange

The goal of the momentum diversion technique is to impose a certain change in velocity vector δ_v to the debris object, causing a decay in orbital energy and sending it to a lower perigee orbit. Thus, the core concept behind this mission is to first rendezvous with a ddo. To accomplish that end, one has to consider all the required phases of orbital transfers for ssc-ddo alignment. In general, such a choreographed maneuver entails several elemental burns along the way. These burns are denoted as a specific delt-v and consist of:

$$d_{v_{total}} = d_{v_i} + d_{v_{H1}} + d_{v_{H2}} + d_{v_{\Omega}} + d_{v_w} + d_{v_{ph}}$$

The first element, d_{v_i} is corresponding to orbital plane change maneuver, aligning the two objects in an equal inclination orbit. The two terms denoted as, $d_{v_{H1}}$ and $d_{v_{H2}}$ are corresponding to the two consecutive Hohman

burns responsible for aligning the ssc's orbit eccentricity and semi-major axis with that of the ddo. The $d_{v_{\Omega}}$ burn will align the orbits in terms of longitude of the ascending node and the $d_{v_{\omega}}$ burn will align the orbit's argument of peri-apsis. By this burn, the ssc is occupying the same orbit as the ddo and the final phasing burn, $d_{v_{ph}}$ will make the rendezvous possible, putting the ssc and ddo on a impact course.

Figure 2 presents overlaid snapshots of the two dimensional model in elliptical orbit throughout the objects' encounter. Here, at point 1, the two objects

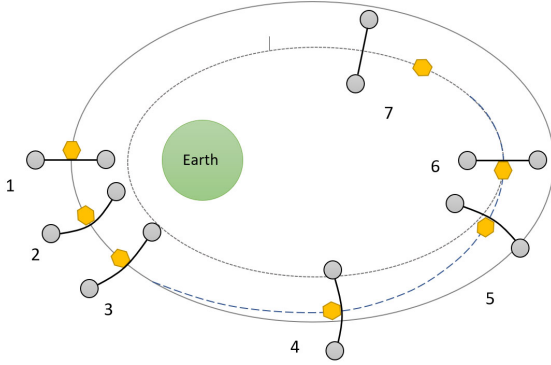


Figure 2: 2-d representation of the dynamical system as overlaid snapshots from rendezvous to departure

make first contact, starting the capture process. This process continues up to point 3, where through natural physical motion and also employing some control logic adjustments, the ddo ends in a secure situation in contact with the membrane. At point 3, the de-orbit burn is activated and through time of arriving at point 4 and going to point 5, the objects decelerate reducing their orbital velocity. Here, the dashed line represents the new trajectory of the objects. At point 5, the ddo is considered de-orbited since the perigee height is reduced to the desired level.

Thus, the ssc commences the departure logic and module spacecrafts move away from one another until the ddo leaves the csm and modules end up in a fully stretched configuration.

Here, in order to demonstrate the phases clearly, half an orbit is shown to be used in the process. In reality, these phases will not take a whole half orbit to complete. In fact, the capture and departure phases take only a few seconds, and since fuel is expensive, the de-orbit burn will also need to be economically feasible. Thus, the de-orbit burn will also take only seconds or minutes. That is, when high I_{sp} thrusters are not included in the design, since using those thrusters introduce the capability of low-thrust trajectories [31]. In theory, it would be possible to design the ssc in such a way that it uses conventional thrust for it's orbit alignment burns, low-thrust technology for it's de-orbit burns, and achieve attitude control through electrical energy by means of

reaction devices. This way, the energy envelope of the ssc could be optimized and enhanced. However, in the current dynamical modeling the assumption is that all thrust is conventional.

Equations of motion: multi-body system

Here, the equations of motion for the multi-body system are presented. In this section, the goal is to derive the dynamical equations of motion for the system in terms of ordinary differential equations. This will pave the path towards smoothly solving the multi-body problem in a computer simulated environment. As shown below, the equations of motion for the rigid bodies involved are quite straightforward. The only complication relates to the flexible part of the ssc, which acts as the capture medium. Here, by the virtue of considering the two dimensional problem, the membrane can be reduced to a flexible string. the dynamics equation for vibration of the string are presented in the coming subsections.

Let us first consider the Newton's second law, or the Euler's first equations for the motion of the debris object. It states that the rate of change of linear momentum of a rigid body is equal to the resultant of all the external forces acting on that body.

$$\frac{dp_d}{dt} = F_{ext}$$

Since $P = mv$ we have:

$$m \frac{dv}{dt} + v \frac{dm}{dt} = F_{ext}$$

Since the debris object has a constant mass, the second term of the equation is zero, so:

$$m \frac{dv}{dt} = F_{ext} \rightarrow m \frac{d^2r}{dt^2} = F_{ext}$$

Which gives us the second order ODE we aimed for.

The module spacecrafts follow the same sets of equations governing the motion of a rigid body except that in reality, since the module spacecrafts burn fuel during the mission, the mass varies and it should be considered for complete understanding of the system dynamics. That said, such variation of mass introduces more complexity and such analysis is outside of the scope here. Thus, the same ODE applies for modules and only the contribution of control forces are added to the external forces.

$$M \frac{d^2r}{dt^2} = F_g + F_t + F_c$$

where $M = m_1 + m_2 + m_3$ and F_g , F_t and F_c respectively stand for gravity, thrust and contact contribution to the net external force.

..... This is placeholder for conservation of angular momentum
.....

$$\frac{dH_d}{dt} = M_{ext}$$

$$H = I\omega$$

$$I \frac{d\omega}{dt} + \omega \frac{dI}{dt} = M_{ext}$$

we assume $\frac{dI}{dt} = 0$ So:

$$I \frac{d\omega}{dt} = M_{ext} \rightarrow I \frac{d^2\theta}{dt^2} = M_{ext}$$

Here, M_{ext} are decomposed to control and contact moments.

$$I \frac{d^2\theta}{dt^2} = M_t + M_c$$

..... This is placeholder
for ending conservation of angular momentum
.....

However, the flexible tether connecting them acts as a continuum and it is more elegant to model it as a continuous system. It will provide us with a smooth and less numerically complicated solution. It also provides good insight into the concept of transforming mechanical energy inside the flexible part of the system. This is achieved by utilizing the Lagrange equations of motion to view the tether as a whole. The sum of all the mechanical energy carried by the tether is presented here.

$$E_m = K_m + U_m$$

here, K_m represents the total kinetic energy and U_m represents the total potential energy.

EOM: natural vibrations equations

Now, let us separate the components of gravity and also the component of center of mass kinetic energy in this equation and isolate the terms corresponding to the vibrations of the tether.

$$E_m = K_{cm} + U_g + K_v + U_v$$

Here, K_{cm} represents the center of mass kinetic energy, and U_g represents the gravity potential. K_v and U_v respectively represent the vibration kinetic energy and the potential energy stored in the form of strain across the tether. Now, assuming a uniform density tether let $\eta(t)$ represent the shape of the string at time t . Now the kinetic energy component of the vibrations is written as:

$$K_v = \int dK_v = \int \frac{1}{2} \rho \dot{\eta}^2 dx$$

Here, $\dot{\eta} = \frac{\partial \eta}{\partial t}$ represents the time rate of change of string shape. The potential energy can also be written as:

$$U_v = \int dU_v = \int T ds = \int T(\sqrt{dx^2 + d\eta^2} - dx)$$

$$= \int T(\sqrt{1 + \eta'^2} - 1) = \int \frac{1}{2} \eta'^2 dx$$

Here $\eta' = \frac{\partial \eta}{\partial x}$ represents the strain of the string along its length. Now that we derived both the kinetic and potential energy expressions for the flexible system, we can now utilize the Lagrange equation to find the equations of motion for the system.

$$L = K_v - U_v = \int \left(\frac{1}{2} \rho \dot{\eta}^2 - \frac{1}{2} T \eta'^2 \right) dx = \int \hat{L} dx$$

where, $\hat{L}(\eta, \dot{\eta}, \eta', x, t)$ represents the lagrangian density of the system. Now by imposing the minimum action principle and utilizing the calculus of variation we have:

$$S = \int L dt = \int \hat{L} dx dt$$

Here, let us consider $\eta \rightarrow \eta + \delta\eta$ as a variation and set the boundary and initial conditions as follows:

$$\delta\eta = 0 \text{ for } t = t_0, t = t_1, x = x_0, x = x_1$$

$$\delta S = \int_{t_0}^{t_1} \int_{x_0}^{x_1} \delta \hat{L} dx dt = 0$$

$$\rightarrow \int_{t_0}^{t_1} \int_{x_0}^{x_1} \left[\frac{\partial \hat{L}}{\partial \eta} \delta\eta + \frac{\partial \hat{L}}{\partial \dot{\eta}} \frac{d}{dt}(\delta\eta) + \frac{\partial \hat{L}}{\partial \eta'} \frac{d}{dx}(\delta\eta) \right] dx dt = 0$$

Now by utilizing the by-part integration technique to the last term inside the integral we reach:

$$\int_{x_0}^{x_1} \frac{\partial \hat{L}}{\partial \eta'} \frac{d}{dx}(\delta\eta) dx = \left[\frac{\partial \hat{L}}{\partial \eta'} \delta\eta \right]_{x_0}^{x_1} - \int_{x_0}^{x_1} \frac{d}{dx} \left(\frac{\partial \hat{L}}{\partial \eta'} \right) \delta\eta dx$$

Where, the boundary condition implies that $\left[\frac{\partial \hat{L}}{\partial \eta'} \delta\eta \right]_{x_0}^{x_1} = 0$. The same technique is applied to the middle term of the aforementioned integral and finally we can write:

$$\delta S = \int_{t_0}^{t_1} \int_{x_0}^{x_1} \left[\frac{\partial \hat{L}}{\partial \eta} - \frac{d}{dt} \left(\frac{\partial \hat{L}}{\partial \dot{\eta}} \right) - \frac{d}{dx} \left(\frac{\partial \hat{L}}{\partial \eta'} \right) \right] \delta\eta dx dt$$

Here, the $\delta S = 0$ if and only if when:

$$\frac{\partial \hat{L}}{\partial \eta} - \frac{d}{dt} \left(\frac{\partial \hat{L}}{\partial \dot{\eta}} \right) - \frac{d}{dx} \left(\frac{\partial \hat{L}}{\partial \eta'} \right) = 0$$

Which is the lagrange equation of motion for the one dimensional flexible system. Now, by replacing $\hat{L} = \frac{1}{2} \rho \dot{\eta}^2 - \frac{1}{2} T \eta'^2$, we get:

$$\frac{\partial \hat{L}}{\partial \eta} = 0, \frac{d}{dt} \left(\frac{\partial \hat{L}}{\partial \dot{\eta}} \right) = \rho \ddot{\eta}, \frac{d}{dx} \left(\frac{\partial \hat{L}}{\partial \eta'} \right) = -T \eta''$$

$$\rightarrow \rho \ddot{\eta} = T \eta''$$

Which can be written as $\frac{\partial^2 \eta}{\partial t^2} = c^2 \frac{\partial^2 \eta}{\partial x^2}$, where $c^2 = \frac{T}{\rho}$, and c represents the speed at which waves of energy propagate through the flexible system.

Mode shapes

The wave equation derived in previous section can be solved by assuming that $\eta(x, t)$ is resulted from multiplying a function of time $\tau(t)$, into a function of x $\varphi(x)$. That is, assuming the shape of string is inherently composed of previously known assumed mode shapes. The mode shapes for the solution of the wave equation has the following form:

$$\varphi_n(x) = \sqrt{\frac{2}{\rho l}} \sin\left(\frac{n\pi}{l} x\right)$$

Where, l represents the length of the string and n represents the number of mode shape. In this section we utilize the assumed mode approach to further simplify the dynamics with the goal of reducing the partial differential equations of the system to a set of ODEs. Based on previous derivations, the equations of motion for the system including the external force can be written as:

$$\rho \frac{\partial^2 \eta}{\partial t^2} - T \frac{\partial^2 \eta}{\partial x^2} = f(x, t)$$

$$B.C.: \eta(x_0, t) = 0, \eta(x_1, t) = 0$$

$$I.C.: \eta(x, 0) = \eta_0(x), \dot{\eta}(x, 0) = \dot{\eta}_0(x)$$

Now we can write the function $\eta(x, t)$ describing the shape of the system as a sum of all decomposed motion elements, each derived as a multiplication of a temporal function $\tau_i(t)$, with a spatial function $\phi_i(x)$.

$$\eta(x, t) = \sum_{i=1}^{\infty} \phi_i(x) \tau_i(t)$$

By inserting it into the wave equation we have:

$$\sum_{i=1}^{\infty} \rho \varphi_i \ddot{\tau}_i - \sum_{i=1}^{\infty} T \varphi_i'' \tau_i = f$$

Here, we continue by multiplying the above equation by the factor φ_j , and then integrate over the length of the string, thus we have:

$$\sum_{i=1}^{\infty} \rho \int_{x_0}^{x_1} \varphi_j \varphi_i \ddot{\tau}_i + \sum_{i=1}^{\infty} T \int_{x_0}^{x_1} \varphi_j \varphi_i'' \tau_i = \int_{x_0}^{x_1} \varphi_j f dx$$

At this point we recall the orthogonality principle which suggest that all of the components of the above equation equals to zero, except for cases where $i = j$, so we reach to the following set of equations:

$$\ddot{\eta}_i + \omega_i^2 \eta_i = Q_i, \quad i = 1, 2, 3, \dots$$

$$\text{Where, } Q_i = \int_{x_0}^{x_1} \varphi_i f dx.$$

Now it's time to work out the external force. for the sake of simplicity, let us consider that the external force (representing the contact force in this case) acts on a specific point and its dynamics can be represented as a δ distribution or in other terms, a factored unit impulse.

$$f(x, t) = F \delta(x - x_c) \delta(t - t_c)$$

$$\delta(x - x_c) = \begin{cases} 0 & x \neq x_c \\ 1 & x = x_c \end{cases}, \quad \int \delta(x - x_c) dx = 1$$

$$\delta(t - t_c) = \begin{cases} 0 & t \neq t_c \\ 1 & t = t_c \end{cases}, \quad \int \delta(t - t_c) dt = 1$$

Now by inserting the mode shapes into $Q_n(t)$ we have:

$$\begin{aligned} Q_n(t) &= F \sqrt{\frac{2}{\rho l}} \int_{x_0}^{x_1} \sin\left(\frac{n\pi}{l} x\right) dx \delta(t - t_c) \\ &= F \sqrt{\frac{2}{\rho l}} \sin\left(\frac{n\pi}{l} x\right) \delta(t - t_c) \end{aligned}$$

Finally, assuming the contact force acts in the mid section of the string at $x = \frac{l}{2}$, we reach to the following natural (un-damped) vibration equation:

$$\ddot{\eta}_n + \omega_n^2 \eta_n = F \sqrt{\frac{2}{\rho l}} \sin\left(\frac{n\pi}{2}\right) \delta(t - t_c)$$

The above equation represents the dynamics of each mode shape, existing in the string and is used to determine the shape through time via numerical integration.

EOM: damped vibrations equations

In reality the string (or generally, the membrane) behaves not only as a natural harmonic oscillator, but also incorporates effects of damping in its vibration. That is, the flexible capture medium will act as a source of energy dissipation based on its mechanical properties. Damping enters the equations of motion as the agent to oppose existing rate of movement, which is to say it is proportional to the time derivative of the state.

$$F_D = -c \dot{\eta}$$

Where F_D represents the force equivalent of the damping agent, and $c = 2\zeta\omega_n$ is the viscous damping coefficient. Thus, the damping term is added to the vibration equations and we have the following ODE to describe the string motion.

$$\ddot{\eta}_n + 2\zeta\omega_n \dot{\eta}_n + \omega_n^2 \eta_n = F \sqrt{\frac{2}{\rho l}} \sin\left(\frac{n\pi}{2}\right) \delta(t - t_c)$$

Contact dynamics

This section provides insight into dynamics of objects through moments of physical contact and introduces a proper mathematical scheme to calculate the contact force between objects during phases of capture, de-orbit and departure. Contact is a complex physical phenomenon which occurs between two or more objects. The surface near the contact region experiences effects of quick energy dissipation and high contact forces, during a short period of time. The dynamics of impact is dependant on various properties of contacting bodies such as geometry, material and relative velocity. In general the process can be decomposed into compression and restitution phases. The objective of impact modelling is to find the after-impact situation, given the initial conditions. The energy loss caused by the motion in the normal direction is famously expressed in terms of a coefficient of restitution, denoted as e . By definition, the coefficient of restitution satisfies the condition $0 \leq e \leq 1$, where $e = 0$ corresponds to a perfect plastic impact and $e = 1$ corresponds to a perfect elastic impact case. The coefficient of restitution is dependant on geometry of the bodies, the relative velocity, mechanical properties of materials, duration of contact and friction. The dependence of e to the relative impact velocity can be related to the ratio of impact time to the period of natural vibration of the system. If this ratio is large, the coefficient of restitution is dominated by the plastic deformations in the contact region and conversely, if the ratio is small, a significant portion of the energy remains in the bodies in the form of vibration. The coefficient of restitution is a high level marker of energy flow throughout the impact phenomena.

Normal force

There are multiple ways of modeling the normal contact force that are categorized to continuous or discrete methods. For a deep analysis of contact force models one can refer to [32]. Here, we utilize the well established continuous contact model, referred to as compliant contact model. It introduces an alternative model for energy dissipation to overcome the problems associated with the spring-dashpot model and at the same time conserving the advantages of the Hert's model [33]. Thus, by considering the non-linear damping model to express the force, we write:

$$F_n = b\delta^p\dot{\delta}^q + k\delta^n$$

where it is standard to set $p = n$ and $q = 1$ [33, 34, 35]. Here, the damping parameter b can be related to the coefficient of restitution. That is because they are both related to the energy dissipation by the impact process. Thus,

$$F_n = b\delta^n\dot{\delta} + k\delta^n$$

Here, n will depend on the contact situation and in this study by hertzian measures, the value of $n = 1.5$ is selected. Moreover, the damping parameter $b = \frac{4}{3}\sqrt{RE^*}$, where

$$E^* = \frac{E_1}{1 - \nu_1^2} + \frac{E_2}{1 - \nu_2^2}$$

Here, E_1 and E_2 represent the young modulus of colliding surfaces, and ν_1 and ν_2 represent the respective Poisson coefficients.

friction

Friction is another complex physical phenomena, present in the impact of bodies. It is a prominent source of energy dissipation and it can be modeled in variety of ways. Most frequently, the Coloumb's friction model is used to describe behavior in impact problems, however, it introduces a discontinuity because of the difference between static and dynamic behaviors.

$$F_f = \mu F_n$$

Here, $\mu = \mu_s$ in static case where the contacting surfaces are not sliding, and $\mu = \mu_k$ in the sliding case. Note that, for most of the cases, $\mu_s > \mu_k$.

Other methods are provided to overcome the discontinuity and also permit a smooth transition from sticking to sliding in [36, 37, 38, 39, 40]. Moreover, [38, 41] presented a bristle model, in which the microscopic action due to friction is modeled based on dynamics of bristles. However, the Coloumb's model, though having the problem of discontinuity will suffice in this study and further exploration of friction models is outside of the scope here.

Module Spacecraft control

In this section, breakdown of control logic is presented and proper control scheme for the mission is provided.

Simulation

In this section the equations of motion for the multi-body system, derived in previous section, are used to build a simulation environment inside a computer. The sets of ODEs governing the motion of the whole system is available and by means of integrating them through time and calculating the present forces and moments in each step, it is possible to simulate the evolution of the dynamics.

There are various software tools available capable of the simulation of the flexible impact problem. Open source software such as blender are used for simulation of cloth like material and impact scenarios relatable to our purpose in this study. Libraries such as bullet and ammo also provide simulation environment for such simulations acting as a physics engine. Tools like blender are specifically designed and optimized for creating and rendering animations, that is the visualization purpose. Libraries like ammo and bullet are built as a physics engine

to create animations and interactive interfaces based on physics principles inside the web browser. However these tools are meant for scientific research, but merely a utility for visualizing results or providing intuition over the problem subject.

In this study we utilize Octave to write and execute scripts that solve the system's ODEs and after calculating the states, produce reports of the simulation case, based on our mathematical modeling of the system.

In order to better understand the system, at first we rely on a two dimensional reductionist model to avoid complexities in three dimensional space. As a result, this section is divided into two subsection. the first part introduces the 2-dimensional dynamics of the scc and ddo interaction. In the second part, the model is augmented to the 3-dimensional dynamics to include the extra dimension and also to incorporate the effects of rotational dynamics. It is worth noting that the main simplification in the 2-D model vs the 3-D, is the role of orientation and complexities associated with the rotation matrices to move between rotating frames. In 2-D the problem is more intuitive and simple to understand. Moreover, the spacecraft's design itself allows for a 2-D representation based on its symmetries.

Later in presenting the 3-D simulation, the mentioned complexities are handled through use of quaternions in solving kinematic equations and also in control logic.

place holder for references in simulation

2-D dynamics

Here, a two dimensional model of the ssc is considered as a means to proof of concept. Later, this model can be augmented to a 3-D representation of the spacecraft system in order to produce more realistic simulations. however, a two dimensional model goes a long way on to demonstrating the de-orbiting capability of the proposed apparatus, while keeping the mathematical and numerical complexity of the problem in favorable status. Since the case is reduced to a planar motion, the ssc can be considered as a two module formation, as opposed to the original four module configuration. Also, the csm can be considered as a flexible tether connecting the two modules, which is the two dimensional projection of a membrane on to a plane, perpendicular to its surface. Here, it is worth noting that these assumptions will affect the behavior of the dynamical system relative to its original three dimensional configuration. For instance, by introducing the uniform tether instead of the membrane, wave propagation attributes will be oversimplified in the two dimensional model. That said, the two dimensional model is very helpful in understanding the overall system dynamics and the way energy flows throughout the mechanical system.

3-D dynamics

Here, a three dimensional model of the ssc is considered as a means to further the demonstration of the proposed technique and also to prove the feasibility of the proposed design.

Results

this section covers the result of simulation

scenario

description of scenario

result

results of simulation scenario

Discussion

mass varies with time as fuel burns.

Findings

The proposed method and design proves to be effective in terms of mission requirements and also it facilitates sustainable removal missions to be scheduled. It has many advantages compared to other momentum exchange methods, in that it does not rely on a solid secured contact scheme to deliver the momentum exchange and to decay the ddo's orbital energy. It carries no extra mass other than the fuel it has to burn for the purpose of de-orbiting the object and maintaining proper deployment configuration throughout the mission.

Conclusion

This study proposed a novel spacecraft system as a means to mitigate the space debris problem. The spacecraft aims to de-orbit several debris objects before running out of fuel, and then rendezvous to a re-fueling station to make itself ready for the next round of dangerous objects in their orbits. This way, we introduce a design and a strategy to effectively counter the dangers of space debris in a sustainable manner. The system consists of four thruster modules, connected through a rigid square frame with a flexible membrane inside. The central region of the membrane will act as capture medium and experiences the contact with the object. By utilizing the two dimensional model of the dynamics, it is shown that the debris object is transported to a new orbit with significantly lower perigee altitude, thus accomplishing the de-orbit criteria.

The proposed system provides a convenient apparatus for engaging with non-collaborating objects and the design is meant to control the object in capture, while simultaneously avoiding to attach or present any attachment vulnerabilities. Simply by placing the membrane opposite to the direction of motion and leaving the flow of de-orbiting energy to the contact force in the base region of the membrane. This is achieved by a choreographed control logic among the four modules. By controlling the thrust on modules, the flexible membrane acts as a sweeping device for space debris. The control logic

for such maneuvering is also presented and implemented to simulate these events. Then after imposing enough energy to the object and burning the necessary fuel to drive the momentum exchange, the departure procedure commences. Here, the modules turn off their thrust, and the flexible membrane throws the object away. The mechanical energy present in the form of potential in the membrane transforms into kinetic energy of the object through contact force, which the object receives as a kick in the centre. These phenomena are also discussed in terms of contact dynamics.

Remarks on thrust technology

References

1. Anz-meador P, Opiela J, Shoots D, and Liou J, eds. History of On-Orbit Satellite Fragmentations, 15th Edition. Houston, Texas: National Aeronautics and Space Administration, 2008
2. Levin E, Carrol J, and Pearson J. The long-term cost of debris removal from leo. 4th International Astronautical Congress, Beijing, China 2013
3. IADC. IADC space debris mitigation guidelines. Inter-Agency Space Debris Coordination Committee. IADC-0201 Rev.1
4. Broadband Series: Regulation of Global Broadband Satellite Communications. International telecommunication union. 2022 Mar 20. Available from: <http://handle.itu.int/11.1002/pub/807b38cc-en> [Accessed on: 2022 Mar 20]
5. Bombardelli C and Pelaez J. Ion beam shepherd for contactless space debris removal. *Journal of Guidance, Control, and Dynamics* 2011; 34(3):916–20. DOI: 10.2514/1.51832
6. Phipps C and al. E. ORION: Clearing near-Earth space debris using a 20-kW, 530-nm, Earth-based, repetitively pulsed laser. *Laser and Particle Beams* 1996; 14(1):1–44. DOI: 10.1017/S0263034600009733
7. Feng G, Li W, and Zhang H. Geomagnetic Energy Approach to Space Debris Deorbiting in a Low Earth Orbit. *International Journal of Aerospace Engineering* 2019. DOI: 10.1155/2019/5876861
8. Trivailo P and Kojima H. Dynamics of the Net Systems, Capturing Space Debris. *Transactions of the Japan Society for Aeronautical and Space Sciences* 2016; 14:57–66. DOI: 10.2322/tastj.14.Pr_57
9. Sharf I, Tomsen B, and Misra A. Experiments and simulation of a net closing mechanism for tether-net capture of space debris. *Acta Astronautica* 2017; 139:332–43
10. Wormnes K, Jong JD, Krag H, and Visentin G. Throw-Nets and Tethers for Robust Space Debris Capture. 64th International Astronautical Congress 2013; Beijing
11. Choi J, Lee D, Jung J, and Kim B. Articulated linkage arms based reliable capture device for janitor satellites. *Acta Astronautica* 2019; 163(8). DOI: 10.1016/j.actaastro.2019.03.002
12. Andrenucci M, Pergola P, and Ruggiero A. Active removal of space debris expanding foam application for active debris removal. ESA 2011
13. Hakima H and Emami M. Assessment of active methods for removal of leo debris. *Acta Astronautica* 2018; 144:225–43
14. Liou J. Active debris removal and the challenges for environment remediation. *Proceedings of the 28th International Symposium on Space Technology and Science* 2012
15. Liou J. Stability of the future leo environment: an iadc comparison study. 6th European Conference on Space Debris, Darmstadt, Germany 2013. DOI: 10.13140/2.1.3595.6487

16. Shan M, Guo J, and Gill E. Review and comparison of active space debris capturing and removal methods. *Progress in Aerospace Sciences* 2016; 80:18–32. DOI: 10.1016/j.paerosci.2015.11.001
17. Priyant M and Kamath S. Review of Active Space Debris Removal Methods. *Acta Astronautica* 2019; 47:194–206
18. Levin E, Pearson J, and Carrol J. Wholesale debris removal from leo. *Acta Astronautica* 2012; 73:100–8
19. Missel J and Mortari D. Removing space debris through sequential captures and ejections. *AIAA Journal of Guidance, Control and Dynamics* 2013; 36(3):743–52
20. Carroll JA. Tether applications in space transportation. *Acta Astronautica* 1986; 13(4):165–74. DOI: 10.1016/0094-5765(86)90061-5
21. Takeichi N and Tachibana N. A tethered plate satellite as a sweeper of small space debris. *Acta Astronautica* 2021; 189:429–36. DOI: 10.1016/j.actaastro.2021.08.051
22. Braun V and al. E. Active debris removal of multiple priority targets. *Advances in Space Research* 2013; 51(9):1638–48. DOI: 10.1016/j.asr.2012.12.003
23. Bérend N and Olive X. Bi-objective optimization of a multiple-target active debris removal mission. *Acta Astronautica* 2016; 122:324–35. DOI: 10.1016/j.actaastro.2016.02.005
24. K.Jorgensen M and Sharf I. Optimal planning for a multiple space debris removal mission using high-accuracy low-thrust transfers. *Acta Astronautica* 2020; 172:56–69. DOI: 10.1016/j.actaastro.2020.03.031
25. Baranov AA, Grishko DA, Khukhrina, and Chen D. Optimal transfer schemes between space debris objects in geostationary orbit. *Acta Astronautica* 2020; 169:23–31. DOI: 10.1016/j.actaastro.2020.01.001
26. Asher ZD, Tragesser S, Kneubel C, and Hudson J. Space Debris Field Removal Using Tether Momentum Exchange. *AAS/AIAA Astrodynamics Specialist Conference* 2018
27. Botta E, Sharf I, and Misra AK. Evaluation of Net Capture of Space Debris in Multiple Mission Scenarios. *26th AAS/AIAA Space Flight Mechanics Meeting* 2016; Napa, CA
28. Flores-Abad A, Maa O, Phamb K, and Ulrichc S. A review of space robotics technologies for on-orbit servicing. *Progress in Aerospace Sciences* 2014; 68:1–26. DOI: 10.1016/j.paerosci.2014.03.002
29. Ellery A, Kreisel J, and Sommer B. The case for robotic on-orbit servicing of spacecraft: Spacecraft reliability is a myth. *Acta Astronautica* 2008; 63(5-6):632–48. DOI: 10.1016/j.actaastro.2008.01.042
30. Zegler F and Kutter B. Evolving to a Depot-Based Space Transportation Architecture. *AIAA SPACE 2010 Conference Exposition* 2010. DOI: 10.2514/6.2010-8638
31. Martinez-Sanchez M and Pollard J. Spacecraft Electric Propulsion—An Overview. *Acta Astronautica* 1998; 14(5):688–99. DOI: 10.2514/2.5331
32. Gilardi G and Sharf I. Literature survey of contact dynamics modelling. *Mechanism and Machine Theory* 2002; 37:1213–39
33. Kenneth Hunt EC. Coefficient of restitution interpreted as damping in vibroimpact. *Journal of Applied Mechanics* 1975. DOI: 10.1115/1.3423596
34. Lankarani H and Nikravesh P. A Contact Force Model With Hysteresis Damping for Impact Analysis of Multi-body Systems. *Journal of Mechanical Design* 1990; 112:369–76. DOI: 10.1115/1.2912617
35. Marhefka DW and Orin DE. A compliant contact model with nonlinear damping for simulation of robotic systems. *IEEE Transactions on Systems, man, and Cybernetics—Part A: Systems and Humans* 1999; 29(6):566–72. DOI: 10.1109/3468.798060
36. Howard WS and Kumar V. A minimum principle for the dynamic analysis of systems with frictional contacts. *Proceedings IEEE International Conference on Robotics and Automation* 1993; 1:437–42. DOI: 10.1109/ROBOT.1993.292211
37. Oden J and Pires E. Nonlocal and Nonlinear Friction Laws and Variational Principles for Contact Problems in Elasticity. *Journal of Applied Mechanics* 1983; 50:67–76. DOI: 10.1115/1.3167019
38. Haessig D and Friedland B. On the Modeling and Simulation of Friction. *Journal of Dynamic Systems, Measurement, and Control* 1991; 113:354–62. DOI: 10.1115/1.2896418
39. Yigit A, Ulsoy A, and Scott R. Spring-dashpot models for the dynamics of a radially rotating beam with impact. *Journal of Sound and Vibrations* 1990; 142:515–25
40. VanVliet J, Sharf I, and Ma O. Experimental validation of contact dynamics simulation of constrained robotic tasks. *The International Journal of Robotics Research* 2000; 19(12):1203–17
41. Ma O. Contact dynamics modelling for the simulation of the Space Station manipulators handling payloads. *IEEE International Conference on Robotics and Automation* 1995; 2:1252–8. DOI: 10.1109/ROBOT.1995.525453
42. Lewis, Hugh, White, Adam E, Crowther, Richard, Stokes, and Hedley. Synergy of debris mitigation and removal. *Acta Astronautica* 2012; 81(1):62–8. DOI: 10.1016/j.actaastro.2012.06.012
43. Witze A. The quest to conquer Earth's space junk problem. *Nature* 2018; 561(7721). DOI: 10.1038/d41586-018-06170-1
44. Sánchez-Arriaga G, Sanmartín J, and Lorenzini E. Comparison of technologies for deorbiting spacecraft from low-earth-orbit at end of mission. *Acta Astronautica* 2017; 138:536–42. DOI: 10.1016/j.actaastro.2016.12.004
45. Celletti A and al. E. Dynamical models and the onset of chaos in space debris. *International Journal of Non-Linear Mechanics* 2017; 90:147–63. DOI: 10.1016/j.ijnonlinmec.2016.12.015
46. Klima R, Bloembergen D, Savani R, and Tuyls K. Space Debris Removal: A Game Theoretic Analysis. *Games* 2016; 7(3). DOI: 10.3390/g7030020

47. Aslanov V and Yudinsev V. Dynamics of large space debris removal using tethered space tug. *Acta Astronautica* 2013; 91(9):149–56
48. Huang P, Hu Z, and Zhang F. Dynamic modelling and coordinated controller designing for the manoeuvrable tether-net space robot system. *Multi-body System Dynamics* 2016; 36:115–41. DOI: 10.1007/s11044-015-9478-3
49. Botta E, Sharf I, and Misra A. Simulation of tethers for capture of space debris and small asteroids. *Acta Astronautica* 2019; 155:448–61. DOI: 10.1016/j.actaastro.2018.07.046
50. Forshaw J and al. E. The active space debris removal mission Remove Debris. Part 1: From concept to launch. *Acta Astronautica* 2020; 168:293–309. DOI: 10.1016/j.actaastro.2019.09.002
51. Zhang X and Liua J. Effective motion planning strategy for space robot capturing targets under consideration of the berth position. *Acta Astronautica* 2018; 148
52. Gołębowski W. Validated simulator for space debris removal with nets and other flexible tethers applications. *Acta Astronautica* 2016; 129:229–40. DOI: 10.1016/j.actaastro.2016.08.037
53. Zhang F and Huang P. Releasing Dynamics and Stability Control of Maneuverable Tethered Space Net. *IEEE/ASME Transactions on Mechatronics* 2016; 22(2):983–93. DOI: 10.1109/TMECH.2016.2628052
54. Anselmo L and Pardini C. The survivability of space tether systems in orbit around the earth. *Acta Astronautica* 2005; 56(3):391–6. DOI: 10.1016/j.actaastro.2004.05.067
55. Forshaw JL. RemoveDEBRIS: An in-orbit active debris removal demonstration mission. *Acta Astronautica* 2016; 127:448–63. DOI: 10.1016/j.actaastro.2016.06.018
56. Aglietti GS and al. E. The active space debris removal mission RemoveDebris. Part 2: In orbit operations. *Acta Astronautica* 2020; 168:310–22. DOI: 10.1016/j.actaastro.2019.09.001
57. Shan M, Guo J, and Gill E. An analysis of the flexibility modeling of a net for space debris removal. *Advances in Space Research* 2020; 65(3):1083–94. DOI: 10.1016/j.asr.2019.10.041
58. Li P, Zhong R, and Lu S. Optimal control scheme of space tethered system for space debris deorbit. *Acta Astronautica* 2019; 165:355–64. DOI: 10.1016/j.actaastro.2019.09.031
59. Sun X and Zhong R. Tether Attachment Point Stabilization of Noncooperative Debris Captured by a Tethered Space System. *Acta Astronautica* 2020. DOI: 10.1016/j.actaastro.2019.12.012
60. Benvenuto R, Salvi S, and Lavagna M. Dynamics analysis and GNC design of flexible systems for space debris active removal. *Acta Astronautica* 2015; 110:247–65. DOI: 10.1016/j.actaastro.2015.01.014
61. Si J, Pang Z, Du Z, and Cheng C. Dynamics modeling and simulation of self-collision of tether-net for space debris removal. *Advances in Space Research* 2019; 64:1675–87. DOI: 10.1016/j.asr.2019.08.006
62. TAKEICHI N, NATORI MC, OKUIZUMI N, and HIGUCHI K. Periodic Solutions and Controls of Tethered Systems in Elliptic Orbits. *Journal of Vibration and Control* 2004; 10(10):1393–413. DOI: 10.1177/1077546304042057
63. Botta E, Sharf I, and Misra A. Contact Dynamics Modeling and Simulation of Tether Nets for Space-Debris Capture. *JOURNAL OF GUIDANCE, CONTROL, AND DYNAMICS* 2017; 40. DOI: 10.2514/1.G000677
64. Shan M, Gill E, and Guo J. Contact Dynamics on Net Capturing of Tumbling Space Debris. *Journal of Guidance, Control, and Dynamics* 2018; 41(9):2060. DOI: 10.2514/1.G003460
65. Kraus P and Kumar V. Compliant contact models for rigid body collisions. *IEEE International Conference on Robotics and Automation* 1987; 2:1382–7. DOI: 10.1109/ROBOT.1997.614330
66. Alves J and al. E. A comparative study of the viscoelastic constitutive models for frictionless contact interfaces in solids. *Mechanism and Machine Theory* 2015; 85:172–88. DOI: 10.1016/j.mechmachtheory.2014.11.020
67. Banerjee A, Chanda A, and Das R. Historical Origin and Recent Development on Normal Directional Impact Models for Rigid Body Contact Simulation: A Critical Review. *Archives of Computational Methods in Engineering* 2016; 24(2). DOI: 10.1007/s11831-016-9164-5
68. Lankarani HM and Nikravesh P. Continuous contact force models for impact analysis in multibody systems. *Nonlinear Dynamics* 1994; 5(2):193–207. DOI: 10.1007/BF00045676
69. Xu W, Liang B, Li C, Liu Y, and Xu Y. Autonomous target capturing of free-floating space robot: Theory and experiments. *Robotica* 2009; 27(3):425–45. DOI: 10.1017/S0263574708004839
70. Shah SV, Sharf I, and Misra AK. Reactionless Path Planning Strategies for Capture of Tumbling Objects in Space Using a Dual-Arm Robotic System. *AIAA Guidance, Navigation, and Control (GNC) Conference* 2013. DOI: 10.2514/6.2013-4521
71. Takeichi N, Natori MC, and Okuizumi N. Fundamental Strategies for Control of a Tethered System in Elliptical Orbits. *Journal of Spacecraft and Rockets* 2003; 40(1):119–25. DOI: 10.2514/2.3924
72. Williams P. Spacecraft Rendezvous on Small Relative Inclination Orbits Using Tethers. *Journal of Spacecraft and Rockets* 2005; 42(6):1047–60. DOI: 10.2514/1.11826
73. Yu B, Jin DP, and Wen H. Analytical deployment control law for a flexible tethered satellite system. *Aerospace Science and Technology* 2017; 66:294–303. DOI: 10.1016/j.ast.2017.02.026

74. Wen H, Jin DP, and Hu HY. Advances in dynamics and control of tethered satellite systems. *Acta Mechanica Sinica* 2008; 24(3):229–41. DOI: 10.1007/s10409-008-0159-9
75. Chen Y, Huang R, He L, Ren X, and Zheng B. Dynamical modelling and control of space tethers: a review of space tether research. *Nonlinear Dynamics* 2014; 77(4):1077–99. DOI: 10.1007/s11071-014-1390-5
76. Rouleau G, Rekleitis I, and L'Archeveque R. Autonomous capture of a tumbling satellite. *Proceedings 2006 IEEE International Conference on Robotics and Automation 2006*; Orlando, Florida. DOI: 10.1109/ROBOT.2006.1642292
77. Bischof B, Kerstein L, and al. E. ROGER - Robotic Geostationary Orbit Restorer. *Science and Technology Series* 2004; 109:183–93. DOI: 10.2514/6.IAC-03-IAA.5.2.08
78. Zhai G and Zhang J. Space Tether Net System for Debris Capture and Removal. *Proceedings of the 2012 4th International Conference on Intelligent Human-Machine Systems and Cybernetics* 2012; 01. DOI: 10.1109/IHMSC.2012.71
79. Hoyt R and al. E. Terminator Tape: A Cost-Effective De-Orbit Module for End-of-Life Disposal of LEO Satellites. *AIAA SPACE 2009 Conference Exposition* 2009; Pasadena, California. DOI: 10.2514/6.2009-6733
80. Aslanov V. Chaos Behavior of Space Debris During Tethered Tow. *Journal of Guidance, Control, and Dynamics* 2015; 39(10):1–7. DOI: 10.2514/1.G001460
81. Zhai G, Zhang J, and Yao Z. Circular Orbit Target Capture Using Space Tether Net System. *Mathematical Problems in Engineering* 2013; 4. DOI: 10.1155/2013/601482
82. Jasper L and Schaub H. Tethered Towing Using Open-Loop Input Shaping and Discrete Thrust Levels. *Acta Astronautica* 2014; 105(1):373–84. DOI: 10.1016/j.actaastro.2014.10.001
83. Sabatini M, Gasbarri P, and Palmerini GB. Elastic Issues and Vibration Reduction in a Tethered Deorbiting Missions. *Advances in Space Research* 2016; 57(9):1951–64. DOI: 10.1016/j.asr.2016.02.010
84. Linskens HTK and Mooij E. Tether Dynamics Analysis and Guidance and Control Design for Active Space-Debris Removal. *Journal of Guidance, Control and Dynamics* 2016; 39(6):1232–43. DOI: 10.2514/1.G001651
85. Cleary S and O'Connor WJ. Control of Space Debris Using an Elastic Tether and Wave-Based Control. *Journal of Guidance, Control and Dynamics* 2016; 39(6):1392–406. DOI: 10.2514/1.G001624
86. Zhai G, Qiu Y, Liang B, and Li C. On-orbit capture with flexible tether-net system. *Acta Astronautica* 2009; 35:613–23. DOI: 10.1016/j.actaastro.2009.03.011
87. Hovell K and Ulrich S. Attitude Stabilization of an Uncooperative Spacecraft in an Orbital Environment using Visco-Elastic Tethers. *AIAA Guidance, Navigation and control Conference* 2016. DOI: 10.2514/6.2016-0641
88. Botta E, Sharf I, Misra AK, and Teichmann M. On the simulation of tether-nets for space debris capture with Vortex Dynamics. *Acta Astronautica* 2016; 123:91–102. DOI: 10.1016/j.actaastro.2016.02.012
89. Liu H, Zhang Q, Yang L, Zhu Y, and Zhang Y. Dynamics of tether-tugging reorbiting with net capture. *Science China Technological Sciences* 2014; 57:2407–17. DOI: 10.1007/s11431-014-5717-8
90. Tibert G and Gärdsback M. Space Webs: Final Report. KTH Engineering Sciences, Royal Institute of Technology: ESA
91. McKenzie DJ. PhD thesis: The dynamics of tethers and space-webs. University of Glasgow, 2010
92. Curtis HD. *Orbital Mechanics for Engineering Students*. 3rd ed. Elsevier, 2014. DOI: 10.1016/C2011-0-69685-1
93. Kaplan M. *Modern Spacecraft Dynamics and Control*. John Wiley and Sons, 1976
94. Jackson R, Ghaednia H, Lee H, Rostami A, and Wang X. *Tribology for Scientists and Engineers - Chapter 3: Contact Mechanics*:93–140. DOI: 10.1007/978-1-4614-1945-7_3
95. Popov VL. *Contact Mechanics and Friction: Physical Principles and Applications*. 1st ed. Berlin: Springer, 2010. DOI: 10.1007/978-3-642-10803-7
96. Johnson KL. *Contact Mechanics*. Cambridge University Press, 1985. DOI: 10.1017/CBO9781139171731